Red-shifted Emission in $Y_3MgSiAl_3O_{12}$: Ce^{3+} Garnet Phosphor for Blue Light Pumped White Light Emitting Diodes

Can He,[1,†] Haipeng Ji,[1,†] Zhaohui Huang,[1,*] Tiesheng Wang,[2] Xiaoguang Zhang,[1] Yangai Liu,[1] Minghao Fang,[1] Xiaowen Wu,[1] Jiaqi Zhang,[3] Xin Min[1,2,*]

[†] C. He and H.P. Ji contributed equally to this paper.

[1]*School of Materials Science and Technology, Beijing Key Laboratory of Materials Utilization of Nonmetallic Minerals and Solid Wastes, National Laboratory of Mineral Materials, China University of Geosciences, Beijing 100083, China*

[2]*Department of Materials Science and Metallurgy, University of Cambridge, 27 Charles Babbage Road, Cambridge CB3 0FS, United Kingdom*

[3]*College of Materials Science and Engineering, Jilin University, Changchun, 130012, China*

**Corresponding author Tel: +86-010-82322186, Fax: +86-010-82322186*

E-mail:huang118@cugb.edu.cn, minx@cugb.edu.cn

Abstract

It is highly desirable to red-shift the emission of $Y_3Al_5O_{12}:Ce^{3+}$ phosphor in order to obtain a warmer correlated color temperature (CCT) in applications for blue light pumped white light emitting diodes (w-LEDs) with high color rendering index (CRI). In this paper, we reported the red-shifted emission of $Y_3MgSiAl_3O_{12}:Ce^{3+}$ garnet phosphor for w-LEDs through a chemical unit co-substituting in solid solution design strategy. The fabrication temperature of the $Y_3MgSiAl_3O_{12}:Ce^{3+}$ powder was optimized at 1600 ºC and its structure, photoluminescence properties, micromorphology, decay curves, quantum yield, as well as the thermal stability of the samples were investigated in details. The as-prepared $Y_3MgSiAl_3O_{12}:Ce^{3+}$ phosphors displayed a broad excitation band ranging from 300 to 520 nm (centered at 450 nm), and presented an intense Ce^{3+} *5d-4f* emission band in the yellow light region (λ_{em}=564 nm, obviously red-shifted away from $Y_3Al_5O_{12}:Ce^{3+}$). This can be explained by the increase of the crystal field splitting in the Ce^{3+} *5d* levels due to the chemical unit co-substitution of Al^{3+}(I) and Al^{3+}(II) ions by Mg^{2+} and Si^{4+} ions. The quantum yield of the $Y_{2.92}MgSiAl_3O_{12}:0.08Ce^{3+}$ phosphor was measured as 61.8%. Further investigation on the packaged w-LEDs lamp by combining $Y_{2.92}MgSiAl_3O_{12}:0.08Ce^{3+}$ phosphors on a blue InGaN chip exhibit a lower CCT and higher CRI compared to the commercial $Y_3Al_5O_{12}$: Ce^{3+} based device, indicating their outstanding strengths for potential applications in w-LEDs.

1 Introduction

Phosphors converted white light emitting diodes (w-LEDs) have recently attracted a growing interest because of their high electrical energy to light energy conversion efficiency, long lifetime, compactness, environmental friendliness and designable features, replacing the conventional incandescent bulbs and fluorescent lamps [1-6]. In addition, because of their excellent performance, w-LEDs have been gradually used in several new application fields such as backlighting of liquid-crystal displays and portable electronics, architectural lighting, car headlights, medical lighting and plant cultivation [7]. Commercial w-LEDs are mainly obtained through the combination of a blue indium gallium nitride (InGaN) chip and yellow phosphors (*e. g.* $Y_3Al_5O_{12}$:Ce (YAG:Ce)) which can be excited by the blue light. [8,9,10] However, these w-LEDs are always limited because of their several disadvantages, such as poor color reproduction, low color rendering index (CRI), and high correlated color temperature (CCT), due to the absence of red light component.

In order to improve the luminescence properties of YAG:Ce phosphors, several studies have been reported on the redshift of emission spectrum through element doping in YAG structure, including the cation-substitution [11-12] and the anion-group -substitution [13]. The results indicated that the emission wavelength mainly depended on changes in lattice parameter and strength of the crystal-field splitting of Ce^{3+} ions during elements substitution [14-15]. Recently, the chemical unit co-substituting solid solution design strategy has been proposed to adjust the emission of YAG:Ce phosphors, such as $(Gd_xY_{3-x})Al_2Ga_3O_{12}:Ce^{3+}$ (x=1,2,3) [16], $YGd_2Al_{5-x}Ga_xO_{12}:Ce^{3+}$ (x=2,3,4) [17], and $Y_2BaAl_4SiO_{12}:Ce^{3+}$ [18]. This approach is considered to have more effects on changing the local or long-range structures of crystal lattice resulting in greater redshift and better CRI value than the one-element substituted YAG:Ce phosphors [19] upon improving YAG's luminescence properties.[20]

To further develop novel phosphors via chemical unit co-substitution with diverse compositions and better CRI, the $Y_3MgSiAl_3O_{12}:Ce^{3+}$ phosphors were designed and prepared here. The Al^{3+}-Al^{3+} couples are supposed to be partly substituted by

Mg^{2+}-Si^{4+} pairs to form a novel $Y_3MgSiAl_3O_{12}$: Ce^{3+} composition without significant changes in phase and crystal structure (different from the previous studies [21] [22]). It is known that all Ce^{3+} ions are surrounded by several AlO_6 octahedral and AlO_4 tetrahedral [23]. Thus, the co-substitution of Al^{3+}-Al^{3+} couples by Mg^{2+}-Si^{4+} pairs can obtain new MgO_6 and AlO_4 coordination polyhedrons, obviously change the local crystal field of Ce^{3+} ion, theoretically enhance its *5d* level splitting and finally red-shift the emission peak into long wavelength regime. Under the excitation at 450 nm, the co-substituted $Y_3MgSiAl_3O_{12}$:Ce^{3+}samples emit intense yellow light centered at 564 nm, further demonstrating the obvious redshift of the emission peaks in comparison to those of the YAG:Ce phosphors (λ_{em}= ~535nm). Meanwhile, a slight redshift of the emission spectrum was observed with the increasing doping concentration of Ce^{3+} ions. To further demonstrate the potential of $Y_{2.92}MgSiAl_3O_{12}$ phosphors for w-LEDs application, the $Y_{2.92}MgSiAl_3O_{12}$: $0.08Ce^{3+}$ phosphors were packaged with the blue LED chip to produce a w-LED lamp with excellent CCT and CRI.

2 Experimental

2.1 Preparation of the $Y_3MgSiAl_3O_{12}$:Ce^{3+} phosphor

The $Y_3MgSiAl_3O_{12}$:Ce^{3+} phosphors were prepared through the conventional high-temperature solid-state reaction under a reducing atmosphere (10% H_2，90% N_2). The raw materials were Y_2O_3 (99.99%), $MgCO_3$ (99.99%), SiO_2 (99.99%), Al_2O_3 (99.99%) and CeO_2 (99.99%). At first, the optimal synthesis temperature was studied. All the raw materials were mixed according to the stoichiometric ratio in their chemical formula. The powder was carefully mixed and ground in an agate mortar, loaded into a corundum crucible and calcined at different temperatures (1450 ºC, 1500 ºC, 1550 ºC, 1600 ºC) for 5 hours under the reducing atmosphere. The powder was melt when the temperature was over 1600 ºC. The heating rate was 8º C/min for T<1000º C, 5 ºC/min for 1000 ºC< T< 1400 ºC and 3 ºC/min T>1400 ºC. The cooling rate was 5º C /min until T<800 ºC. When the sample was naturally cooled down to room temperature, a yellow $Y_{2.96}MgSiAl_3O_{12}$:$0.04Ce^{3+}$ powder sample was obtained after grinding. The Ce^{3+}-doped phosphors $Y_{3-x}MgSiAl_3O_{12}$:xCe^{3+}

with x= 0.04, 0.06 or 0.08 were prepared through the same procedure at the optimum calcination temperature (1600 ºC).

2.2 Package of the w-LEDs Lamp

The $Y_{2.92}MgSiAl_3O_{12}:0.08Ce^{3+}$ sample was selected to fabricate the w-LEDs lamp. Initially, 1.4 g of glue A was added into a 10 mL beaker under stirring. 1g $Y_{2.92}MgSiAl_3O_{12}:0.08Ce^{3+}$ powder was then added under continuous stirring. Just after 5.6 g of curing agent B was added into the beaker under stirring, an ultrasonic bath (30 min) was used to expel air bubbles out of the glue mixture. An unpackaged LEDs chip was used for the experiment and the cover on the chip was removed. A small amount of the glue mixture was dropped on the chip in the groove until the dew-shaped glue emerged from the groove. Finally, the packaged w-LEDs lamp was put in a vacuum oven for drying (at 65 ºC for 40 min and later at 135 ºC for 80 min). After the oven cooled to room temperature, the w-LEDs lamp was taken out for tests.

2.3 Characterization

The *X*-ray diffraction (XRD) data of the as-prepared samples was collected on an *X*-ray powder diffractometer (SHIMADZU, XRD-6000) using Cu Kα radiation (λ=0.15406 nm), under operating electric voltage and current of 40 kV and 30 mA, respectively. The diffraction data was collected with a scanning speed of 8º (2θ)/min in the 2θ range from 10º to 80º. The photoluminescence excitation (PLE) spectra and photoluminescence (PL) spectra were measured using a fluorescence spectrophotometer (F-4600, HITACHI, Japan), under an operating voltage of 400 V at room temperature. In addition, a 150 W Xe lamp was used as the excitation source. The scanning electron microscope (SEM) used for The micro-morphology of the as-prepared $Y_{2.92}MgSiAl_3O_{12}:0.08Ce^{3+}$ powder is S-4800, Hitachi, Japan. The PL decay curves were obtained through a steady state/transient fluorescence spectrometer (FLS-980, Edinburgh, UK) with an excitation source, under a pulsed laser radiation of 450 nm. The PL quantum yield (QY) was recorded using a 10 inch integrating sphere (Labsphere Inc., LMS-100) attached with a multi-channel CCD detector (Ocean Optics Inc., USB QE Pro-65). For the investigation of emission stability with the temperature (298–473 K), the temperature-dependent luminescence intensity was

monitored on the same spectrophotometer combined with a computer-controlled electric heater (TAP02). The room temperature electroluminescence (EL) spectrum of the w-LEDs lamp packaged with $Y_{2.92}MgSiAl_3O_{12}:0.08Ce^{3+}$ phosphor was also recorded with the same fluorescence spectrophotometer but without the Xe lamp excitation.

3 Results and discussion

Fig. 1(a) shows the crystal structure of $Y_3Al_5O_{12}$ typical unit cell and the substitution of Mg^{2+}–Si^{4+} pairs. When Mg^{2+} (*CN*= 6, R_{Mg}^{2+} = 0.720 Å) and Si^{4+} (*CN*= 4, R_{Si}^{4+} = 0.260 Å) ions are introduced into the YAG structure, they occupy the sites of the Al^{3+} (I) ions (*CN*= 6, R_{Al}^{3+} = 0.535 Å) and Al^{3+}(II) ions (*CN*= 4, R_{Al}^{4+} = 0.390 Å) , respectively (Fig. 1(a)). The aluminum-oxygen octahedron and the aluminum-oxygen tetrahedron are partly substituted by magnesium-oxygen octahedron and silicon-oxygen tetrahedron to form the $Y_3MgSiAl_3O_{12}:Ce^{3+}$ compound, similar to other co-substitution systems we investigated previously [24 25]. Due to the ion size and charge compensation, the crystal structure and neutrality are maintained. Similarly, the substitution of Y^{3+} by Ce^{3+} ions, due to the same valence (+3) and similar ionic radius (*CN*=8, R_{Ce}^{3+} = 1.143 Å, R_Y^{3+} = 1.019 Å), will not change the YAG crystal structure, which have already been reported by extensive literatures[26-28].

XRD patterns for our $Y_3MgSiAl_3O_{12}:Ce^{3+}$ phosphors displayed in Fig. S1 indicate that the temperature for optimized synthesis is 1600 ºC. The $Y_{3-x}MgSiAl_3O_{12}:xCe^{3+}$ phosphors with different Ce^{3+} doping contents were then obtained at the optimal temperature for 5 hours. The XRD patterns of $Y_{3-x}MgSiAl_3O_{12}:xCe^{3+}$ indicate that the obtained samples have single phase and the doped Ce^{3+} ions cannot influence the crystalline structure of the host material significantly (Fig. 1(b)). SEM images (Fig. 1(c) and Fig. S2) show a spherical morphology of $Y_{2.92}MgSiAl_3O_{12}:0.08Ce^{3+}$ phosphors (diameter = 1-3 μm, which is suitable for the requirement of w-LEDs [29-30]) due to the intrinsic crystal properties of the cubic garnet structure.

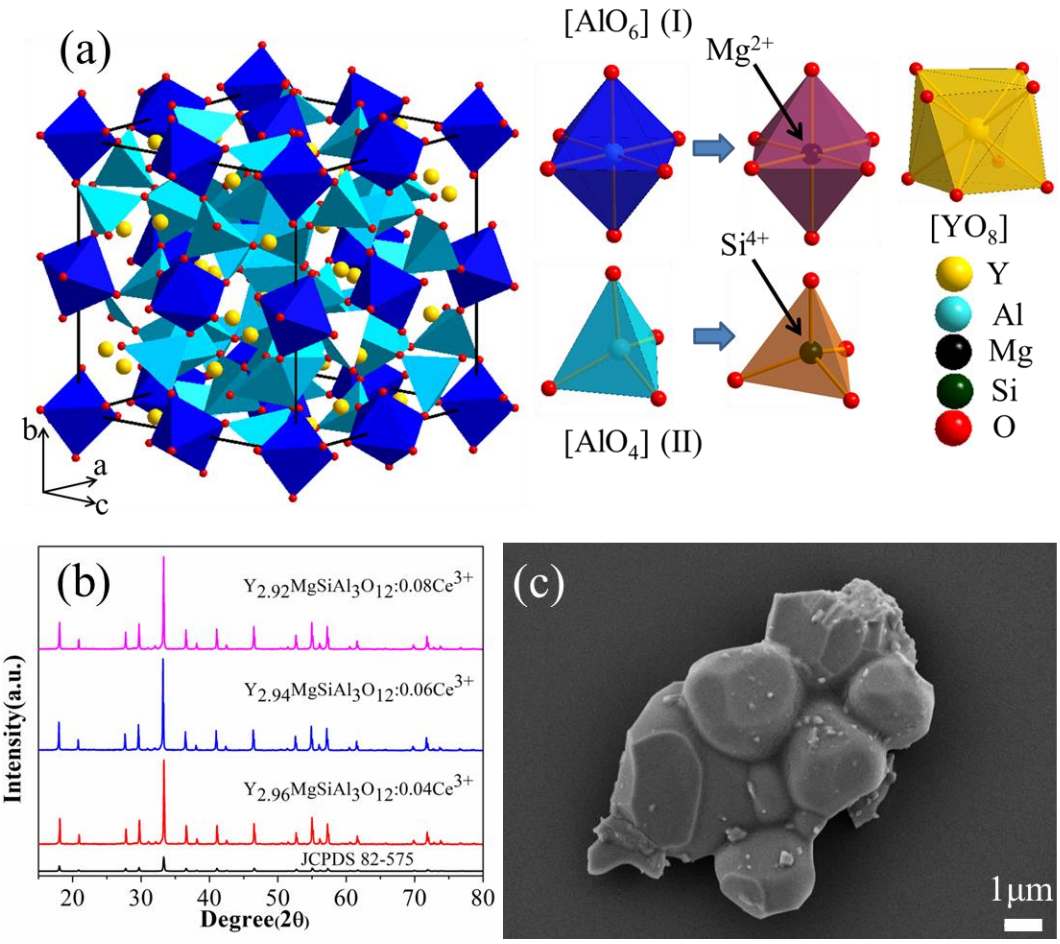

Fig. 1 a) Crystal structure of $Y_3Al_5O_{12}$ and the substitution of Al^{3+}–Al^{3+} by Mg^{2+}–Si^{4+} pair. The $Y_3Al_5O_{12}$ typical garnet unit cell consists of [YO_8] dodecahedron, [AlO_6] octahedron, and [AlO_4] tetrahedron, which belongs to the space group $Ia\bar{3}d$ (no. 230) with the cell parameters of $a=b=c$=12.024(1) Å, V=1738.432(1) Å^3 and Z=8. b) XRD patterns of various concentrations of Ce^{3+}-doped $Y_3MgSiAl_3O_{12}$ samples (x= 0.04, 0.06, and 0.08) and standard data from $Y_3Al_5O_{12}$ (JCPDS card No. 82-575). Almost all of the diffraction peaks are assigned to the garnet structure of $Y_3Al_5O_{12}$ and match well with the standard JCPDS card. c) Typical SEM image of $Y_{2.92}MgSiAl_3O_{12}$:0.08Ce^{3+} phosphor

The excitation spectra (Fig. 2(a)) are nearly identical and they are composed of the half-peak of the monitoring wavelength at ~281 nm and two broad excitation bands from Ce^{3+} ions located in the 300–380 nm ($4f\rightarrow5d_2$) and 380–525 nm ($4f\rightarrow5d_1$) regions. Meanwhile, all the samples show a maximum excitation peak at ~450 nm,

which indicates that the $Y_{3-x}MgSiAl_3O_{12}$:xCe^{3+} phosphors can be efficiently excited with a commercial blue InGaN chip [31]. The two broad excitation bands located at 320 and 450 nm are attributed to the transitions of Ce^{3+} ions from the 4*f* ground state to excited levels $^2T_{2g}$ ($5d_2$) and ^2E_g ($5d_1$), respectively [32]. The emission spectra of the $Y_{3-x}MgSiAl_3O_{12}$:xCe^{3+} phosphors demonstrate that all the phosphors exhibit a yellow emission band from 475 to 725 nm (Fig. 2(b)). Moreover, under excitation at 450 nm, the emission band successfully achieved an obvious red-shift from 535 nm of $Y_{2.96}Al_5O_{12}$: $0.04Ce^{3+}$ to 561 nm of $Y_{2.96}MgSiAl_3O_{12}$: $0.04Ce^{3+}$, as shown in Fig. S3. The insets of Fig. 2(b) show the photos of the as-prepared $Y_{3-x}MgSiAl_3O_{12}$:xCe^{3+} phosphors, all of which present a bright yellow color in daylight. Meanwhile, the emission spectra of all the samples are asymmetric due to the energy transition from the bottom of Ce^{3+} 5*d* excited state to the two 4*f* ground states ($^2F_{5/2}$ and $^2F_{7/2}$). The emission intensity increases with Ce^{3+} ions concentration, reaches the maximum at the doping concentration x=0.08. In addition, a slight red-shift of the emission peaks is observed (from 561 nm to 564 nm, Fig S4) with the increase of the Ce^{3+} ions doping concentration, which suggests an enhanced crystal field splitting of the Ce^{3+} 5*d* levels [33].

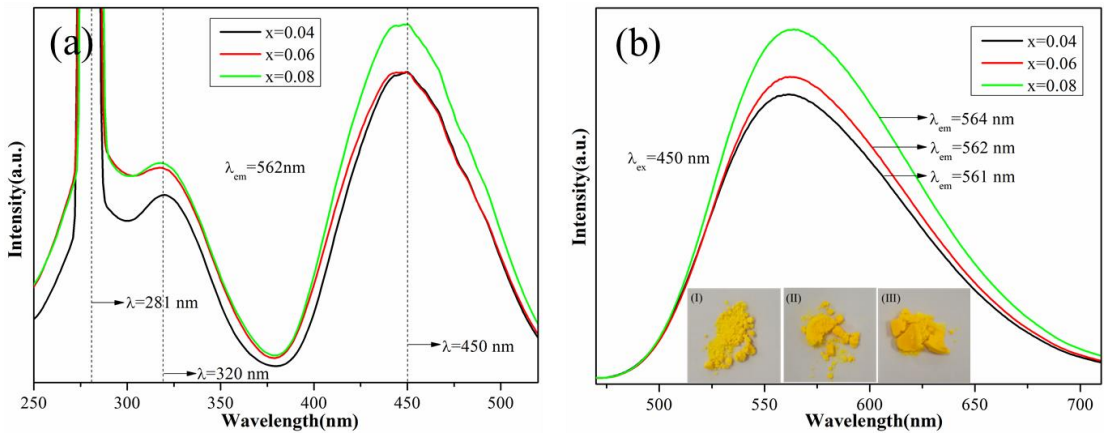

Fig.2 (a) PLE spectra of $Y_{3-x}MgSiAl_3O_{12}$: xCe^{3+} (x= 0.04, 0.06 and 0.08) phosphors monitored at 562 nm emission; (b) PL spectra of $Y_{3-x}MgSiAl_3O_{12}$: xCe^{3+} (x= 0.04, 0.06 and 0.08) phosphors under the excitation of 450 nm. The inset images show the photos of the as-prepared phosphors (I: x=0.04, II: x=0.06, III: x=0.08) under daylight.

In order to further understand the mechanism of the redshift emission, each emission peaks for the $Y_{3-x}MgSiAl_3O_{12}$:xCe^{3+} phosphors are de-convoluted into two peaks by Gaussian peak separation as shown in Fig. 3(a). Meanwhile, the energy level scheme of Ce^{3+} ion is also obtained to understand the Ce^{3+} energy level distribution in $Y_{2.92}MgSiAl_3O_{12}$:$0.08Ce^{3+}$ phosphor (Fig. 3(b)). The 4*f* electronic ground level of Ce^{3+} ions splits into two spectral branches due to spin-orbit (S.O.) coupling, *i.e.* $^2F_{7/2}$ and $^2F_{5/2}$. The excited state 5*d* level is affected by the crystal field and therefore splits into 2 to 5 energy levels [34]. The PLE spectrum of $Y_3Al_5O_{12}$:Ce^{3+} consists of two peaks located at ~340 nm (29412 cm^{-1}) and ~450 nm (22222 cm^{-1}) [35], while the excitation peaks of $Y_{2.92}MgSiAl_3O_{12}$:$0.08Ce^{3+}$ were centered at 320 nm (31250 cm^{-1}) and 450 nm (22222 cm^{-1}). Thus the energy difference between the $5d_2$ and $^2F_{5/2}$ levels is increased by 1838 cm^{-1}. While, the energy difference between $5d_1$ and $^2F_{5/2}$ is 18285 cm^{-1} and the energy difference between $5d_1$ and $^2F_{7/2}$ is 17012 cm^{-1}. According to the Gaussian peak separation, the Stokes Shift of the $Y_{2.92}MgSiAl_3O_{12}$:$0.08Ce^{3+}$ phosphor is 3937 cm^{-1}. The substitution of Al^{3+}(I) and Al^{3+}(II) ions by Mg^{2+} and Si^{4+} ions in the $Y_{3-x}MgSiAl_3O_{12}$:xCe^{3+} samples enhances the local crystal field, resulting in a greater splitting of the excited 5*d* level states of Ce^{3+} ions. In addition, the broadening of the energy transition bands indicates a higher diversity of local environments of Ce^{3+} ions in highly doped Mg–Si garnets. When the Ce^{3+} ion occupies an ideal cubic symmetrical lattice, the 5*d* energy level will split into two groups of excited states ($5d_1$ and $5d_2$). When the lattice is distorted , the two excited energy levels can further split into five energy levels [36] [37]. In $Y_{3-x}MgSiAl_3O_{12}$:xCe^{3+} solid solutions, the substitution of Al^{3+}(I) and Al^{3+}(II) ions by Mg^{2+} and Si^{4+} ions enhances the lattice distortion, then the energy gaps between the five energy levels further increase [38]. The energy gap between the lowest excited state level and the ground state level decreases accordingly, leading to the shift of the emission spectrum to the lower energy side, *i.e.* the red-shift of the emission spectrum.

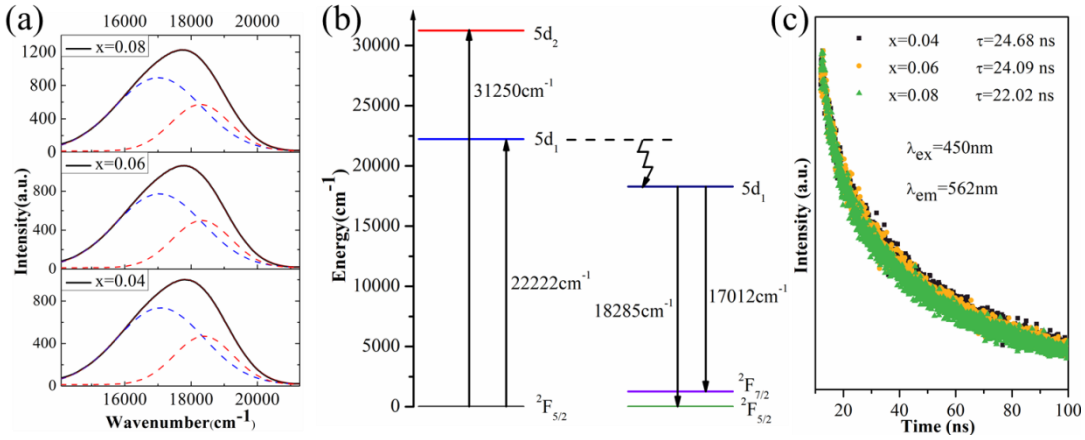

Fig.3 (a) Gaussian deconvolution of $Y_{3-x}MgSiAl_3O_{12}:xCe^{3+}$ phosphors; (b) Energy levels scheme of Ce^{3+} ion in $Y_{2.92}MgSiAl_3O_{12}:0.08Ce^{3+}$ phosphor; (c) Decay curves for the $Y_{3-x}MgSiAl_3O_{12}:xCe^{3+}$ (x=0.04, 0.06, 0.08) phosphors monitored at 562 nm and excited at 450 nm.

Fig. 3(c) shows the PL decay curves of the $Y_{3-x}MgSiAl_3O_{12}$: xCe^{3+} phosphors recorded at room temperature. According to the decay behavior of Ce^{3+} in garnet structure, the corresponding luminescence decay curves were well fitted with the single exponential function by the following equation [39]:

$$I(t) = I_0 + A_1 * exp(-t/\tau) \quad (1)$$

where t is the time, $I(t)$ is the luminescence intensity at the time t, I_0 and A_1 are constants, and τ is the radiative decay time. The PL decay fitting parameters of the samples are presented in Table S1. The lifetimes of the as-prepared $Y_{3-x}MgSiAl_3O_{12}$: xCe^{3+} samples were calculated to be 24.68 ns (x=0.04), 24.09 ns (x=0.06), and 22.02 ns (x=0.08), which decreases with the increase of Ce^{3+} ion concentration inferring that the diminished lifetime is mainly resulted from the increasing interaction between adjacent Ce^{3+} ions at high Ce^{3+} doping concentration [40]. Compared with other YAG: Ce based phosphor [41,42], $Y_3MgSiAl_3O_{12}$: Ce^{3+} obtains a shorter PL lifetime due to the seriously distorted lattice [43] led by the the Mg-Si pairs chemical unit co-substitution.

In general, sufficient thermal stability is important for phosphors to be further used in w-LED applications.[44] As shown in Fig. S5, the luminescence intensity decreases with the increasing temperature under the excitation of 450 nm. The

intensity of the $Y_{2.92}MgSiAl_3O_{12}:0.08Ce^{3+}$ phosphor at 373 K can maintain about 64.8% of that at room temperature. This indicates that the yellow-emitting $Y_3MgSiAl_3O_{12}:Ce^{3+}$ phosphor presents a reasonable thermal stability for low-powered LEDs applications. Moreover, the maximum emission is nearly at the same wavelength upon temperature variation, which can also be beneficial for providing a stable luminous performance of the w-LED lamps. Furthermore, the quantum yield (QY) of the selected $Y_{2.92}MgSiAl_3O_{12}:0.08Ce^{3+}$ phosphor was also measured as 61.8%. As a potential candidate for a w-LED phosphor, the as-presented phosphor shows the competitive QY for potential practical applications [45].

To demonstrate the luminous effect of the as-prepared phosphors for potential practical application, $Y_{2.92}MgSiAl_3O_{12}:0.08Ce^{3+}$ was incorporated in a w-LED lamp. As a specific package process shown in Fig. S6, a commercial blue InGaN chip (λ_{em}=460 nm) was used for packaging experiment and a commercial AB glue with glue A and hardener B was used as a binder. Fig. 4(a) shows the EL spectrum of packaged lamp driven by a 300 mA current, which consists of the blue and yellow light from the InGaN chip and as-prepared phosphors respectively. As shown in Fig. 4(b), the corresponding CIE color coordinates of the packaged w-LEDs lamp are calculated to be (0.3450, 0.3320), which are similar to the ideal white chromaticity coordinate (0.3333, 0.3333) of the National Television Standard Committee system [46]. The inset photo in Fig. 4(b) (top right) display an intense white light emitting for the packaged lamp with the warm white light (4882 K) and high CRI (Ra) value of 90 (Table 1). The CCT and CRI of the lamp packaged with the as-prepared $Y_3MgSiAl_3O_{12}$: Ce^{3+} phosphor are superior to the w-LED lamp packaged with commercial $Y_3Al_5O_{12}:Ce^{3+}$ phosphor (Table 1). Moreover, the low CCT and high CRI of the lamp are also comparable to those for the w-LED lamp packaged with the combination of $Y_3Al_5O_{12}:Ce^{3+}$ and commercial red phosphor. The above-mentioned results confirm that the luminescence properties of $Y_3Al_5O_{12}:Ce^{3+}$ can be significantly improved by the Mg-Si pairs chemical unit co-substitution and demonstrate its potential for warm white light illumination.

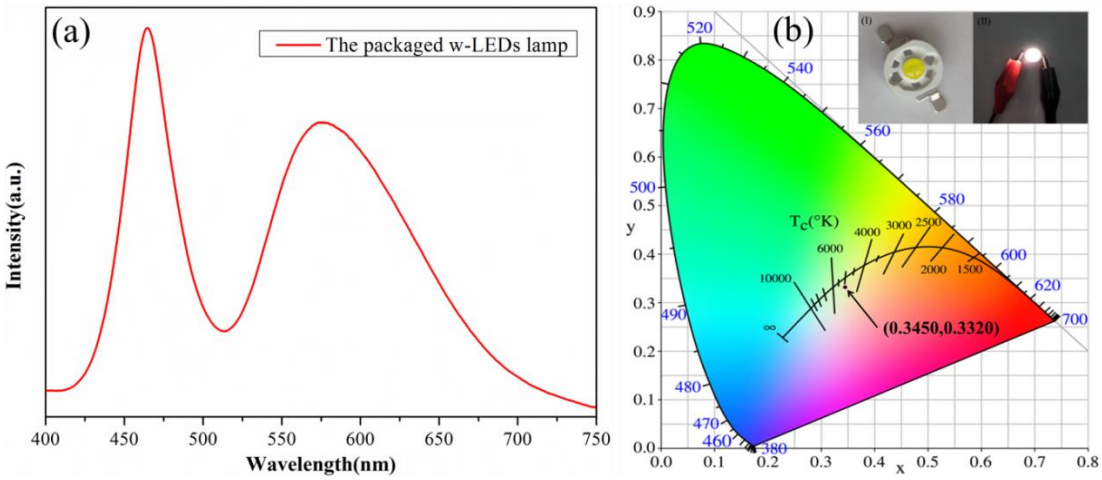

Fig.4 a) EL spectrum of the as-prepared phosphor $Y_{2.92}MgSiAl_3O_{12}:0.08Ce^{3+}$ in conjunction with the 460 nm InGaN chip. b) CIE color coordinates of the packaged w-LED lamps, and the inset images present the photograph of the packaged lamp and its illumination at an operating voltage of 3 V.

Table 1 CCT and CRI (Ra) of the w-LEDs lamps packaged with different phosphors.

phosphor	λ_{ex}(LED) nm	CCT (K)	CRI	Ref
$Y_3MgSiAl_3O_{12}$: Ce^{3+}	460	4882	90	--
$Y_3Al_5O_{12}$:Ce^{3+}	460	5600	71	[47]
$Y_3Al_5O_{12}$:Ce^{3+}, CaS:Eu^{2+}	460	5500	92	[48]
$Y_3Al_5O_{12}$:Ce^{3+}, $Sr_2Si_5N_8$:Eu^{2+}	460	2900	80	[49]

4 Conclusions

In conclusion, the yellow-emitting garnet structure $Y_3MgSiAl_3O_{12}$:Ce^{3+} phosphors were rationally designed and prepared via chemical unit co-substituting solid solution strategy. The temperature for fabricating $Y_3MgSiAl_3O_{12}$ is optimized to be 1600 ºC through a high-temperature solid phase method. The XRD results matches the successful substitution of Al^{3+}(I) and Al^{3+}(II) ions by Mg^{2+} and Si^{4+} ions preserves the crystal structure of YAG. The $Y_3MgSiAl_3O_{12}$: $x$$Ce^{3+}$ phosphors exhibit a yellow emission band under the excitation at 450 nm, centered at 561 nm (x=0.04), 562 nm (x=0.06) and 564 nm (x=0.08) respectively. The characteristic emission band

corresponds to the energy transition of the Ce^{3+} 5d excited state bottom to the 4*f* ground states ($^2F_{5/2}$ and $^2F_{7/2}$). In addition, compared to the emission spectrum of $Y_3Al_5O_{12}:Ce^{3+}$ phosphor, $Y_3MgSiAl_3O_{12}:Ce^{3+}$ phosphors emit yellow light obviously red-shifted from 535 to 564 nm, due to the increasing crystal field splitting of the Ce^{3+} 5d levels by the Mg^{2+}-Si^{4+} pairs co-substitution. Furthermore, the lifetimes of $Y_3MgSiAl_3O_{12}$: $x Ce^{3+}$ phosphors were calculated to be 24.68 ns (x=0.04), 24.09 ns (x=0.06), 22.02 ns (x=0.08), and the quantum yield (QY) of the selected $Y_{2.92}MgSiAl_3O_{12}:0.08Ce^{3+}$ phosphor was measured to be 61.8%. These results indicate that chemical unit co-substituting solid solution design strategy is an effective method to adjust the emission spectra of $Y_3Al_5O_{12}:Ce^{3+}$. The well-packaged w-LED lamp exhibits a warm white light (4882 K) and a high CRI (Ra) value of 90, promising the application of $Y_3MgSiAl_3O_{12}:Ce^{3+}$ phosphors as blue-excited yellow-emitting components for w-LEDs.

Supporting Information

XRD patterns of $Y_{2.96}MgSiAl_3O_{12}:0.04Ce^{3+}$ samples synthesized at various sintering temperatures, SEM images of $Y_{2.92}MgSiAl_3O_{12}:0.08Ce^{3+}$ phosphors, normalized PL spectra of $Y_{2.96}Al_5O_{12}$: $0.04Ce^{3+}$ and $Y_{2.96}MgSiAl_3O_{12}$: $0.04Ce^{3+}$ phosphors, emission spectra of $Y_{2.92}MgSiAl_3O_{12}:0.08Ce^{3+}$ phosphor under different test temperatures, pack aging process diagram of the w-LED lamp, fitting parameters of the PL decay curves.

Acknowledgements

This present work was supported by the Fundamental Research Funds for the Central Universities for financial support (Grant No. 2652017362), the National Natural Science Foundations of China (Grant No. 51472222, 51372232).

Author contributions

C. He and H. P. Ji contributed equally to this paper.C. He, H.P. Ji, Z.H. Huang and X. Min conceived and designed the experiments. C. He and H.P. Ji carried out the experiments. C. He, H.P. Ji, T.S. Wang, X.G. Zhang, Y.G. Liu, M.H. Fang, X.W. Wu,

J.Q. Zhang, and X. Min analyzed the data and discussed the results. C. He and H.P. Ji wrote the paper together with input from all the authors.

Additional information

Competing financial interests: The authors declare no competing financial interests.

References

1. Chen, W.; Zhang, J., Using Nanoparticles to Enable Simultaneous Radiation and Photodynamic Therapies for Cancer Treatment. *J. Nanosci. Nanotechno.* **2006**, *6*, 1159-1166.

2. Liu, Y.; Chen, W.; Wang, S.; Joly, A. G., Investigation of Water-Soluble X-Ray Luminescence Nanoparticles for Photodynamic Activation. *Appl. Phys. Lett.* **2008**, *92*, 043901-043903.

3. Zou, X.; Yao, M.; Ma, L.; Hossu, M.; Han, X.; Juzenas, P.; Chen, W., X-Ray-Induced Nanoparticle-Based Photodynamic Therapy of Cancer. *Nanomedicine* **2014**, *9*, 2339-2351.

4. Bachmann, V.; Ronda, C.; Meijerink, A., Temperature Quenching of Yellow Ce^{3+} Luminescence in YAG:Ce. *Chem. Mater.* **2009**, *21*, 2077-2084.

5. Zhong, J.; Zhuang, W.; Xing, X.; Wang, L.; Li, Y.; Zheng, Y.; Liu, R.; Liu, Y.; Hu, Y., Blue-Shift of Spectrum and Enhanced Luminescent Properties of YAG: Ce^{3+} Phosphor Induced by Small Amount of La^{3+} Incorporation. *J. Alloy. Compd.* **2016**, *674*, 93-97.

6. Nien, Y. T.; You, J. K., Improved Thermal Quenching of $Y_3Al_5O_{12}$: Ce Phosphor Ceramics with Silica Addition. *J. Alloy. Compd.* **2016**, *678*, 1-4.

7. Ji, H.; Cho, Y.; Wang, L.; Hirosaki, N.; Molokeev, M. S.; Huang, Z.; Xie, R.-J., Phase Formation of $(Y,Ce)_2BaAl_4SiO_{12}$ Yellow Microcrystal-Glass Phosphor for Blue LED Pumped White Lighting. *Ceram. Int.* **2017**, *43*, 6425-6429.

8. Abd, H. R.; Hassan, Z.; Ahmed, N. M.; Omar, A. F.; Alsultany, F. H.; Yusof, Y., Laser-Induced Solution Combustion of Nano-$Y_{2.96}Al_5O_{12}$: 0.04Ce Phosphors and Their Fluorescent Properties for White Light Conversion. *J. Alloy. Compd.* **2017**, *711*, 42-50.

9. Tang, Y.; Zhou, S.; Chen, C.; Yi, X.; Feng, Y.; Lin, H.; Zhang, S., Composite Phase Ceramic Phosphor of Al_2O_3-Ce:YAG for High Efficiency Light Emitting. *Opt. Express* **2015**, *23*, 17923-17928.

10. Xia, Z.; Liu, Q., Progress in Discovery and Structural Design of Color Conversion Phosphors

for LEDs. *Prog. Mater. Sci.* **2016**, *84*, 59-117.

11. Zhang, M.; Li, B.; Yang, Y.; Chen, S.; He, X.; Zhao, F.; Zeng, Q., Correlation between Structure and Optical Properties in $(Y,Lu)_3Al_5O_{12}:Ce^{3+}$ Solid Solutions. *J. Phys. D Appl. Phys.* **2016**, *49*, 415101.

12. Li, K.; Shucai, G.; Guangyan, H.; Jilin, Z., Relationship between Crystal Structure and Luminescence Properties of $(Y_{0.96-x}Ln_xCe_{0.04})_3Al_5O_{12}$ (Ln = Gd, La, Lu) Phosphors. *J. Rare. Earth.* **2007**, *25*, 692-696.

13. Zorenko, Y.; Zorenko, T.; Malinowski, P.; Sidletskiy, O.; Neicheva, S., Luminescent Properties of $Y_3Al_{5-x}Ga_xO_{12}$:Ce Crystals. *J. Lumin.* **2014**, *156*, 102-107.

14. Ji, H.; Wang, L.; Molokeev, M. S.; Hirosaki, N.; Huang, Z.; Xia, Z.; Kate, O. M. T.; Liu, L.; Xie, R., New Garnet Structure Phosphors, $Lu_{3-x}Y_xMgAl_3SiO_{12}$:Ce^{3+} (x= 0–3), Developed by Solid Solution Design. *J. Mater. Chem. C* **2016**, *4*, 2359-2366.

15. Pan, Z.; Li, W.; Xu, Y.; Hu, Q.; Zheng, Y., Structure and Redshift of Ce Emission in Anisotropically Expanded Garnet Phosphor MgYAlSiO :Ce. *Rsc Adv.* **2016**, *6*, 20458-20466.

16. Chewpraditkul, W.; Pattanaboonmee, N.; Sakthong, O.; Chewpraditkul, W.; Szczesniak, T.; Moszynski, M.; Kamada, K.; Yoshikawa, A.; Nikl, M., Luminescence and Scintillation Characteristics of $(Gd_xY_{3-x})Al_2Ga_3O_{12}$:Ce (x = 1,2,3) Single Crystals. *Opt. Mater.* **2018**, *76*, 162-168.

17. Chewpraditkul, W., et al., Optical and Scintillation Properties of Ce^{3+} -Doped $YGd_2Al_{5-x}Ga_xO_{12}$ (x =2,3,4) Single Crystal Scintillators. *J. Lumin.* **2016**, *169*, 43-50.

18. Ji, H.; Wang, L.; Cho, Y.; Hirosaki, N.; Molokeev, M. S.; Xia, Z.; Huang, Z.; Xie, R. J., New $Y_2BaAl_4SiO_{12}$: Ce^{3+} Yellow Microcrystal-Glass Powder Phosphor with High Thermal Emission Stability. *J. Mater. Chem. C* **2016**, *4*, 9872-9878.

19. Wu, H.; Yang, C.; Zhang, Z.; Tang, Y., Photoluminescence and Thermoluminescence of Ce^{3+} Incorporated $Y_3Al_5O_{12}$ Synthesized by Rapid Combustion. *Optik-Int. J. Light Electron Opt.* **2016**, *127*, 1368-1371.

20. Katelnikovas, A.; Bettentrup, H.; Uhlich, D.; Sakirzanovas, S.; Jüstel, T.; Kareiva, A., Synthesis and Optical Properties of Ce^{3+}-Doped $Y_3Mg_2AlSi_2O_{12}$ Phosphors. *J. Lumin.* **2009**, *129*, 1356-1361.

21. Ji, H.; Wang, L.; Cho, Y.; Hirosaki, N.; Molokeev, M. S.; Xia, Z.; Huang, Z.; Xie, R. J., New

$Y_2BaAl_4SiO_{12}:Ce^{3+}$ Yellow Microcrystal-Glass Powder Phosphor with High Thermal Emission Stability. *J. Mater. Chem. C* **2016**, *4*, 9872-9878.

22. Pan, Z.; Chen, J.; Wu, H.; Li, W., Red Emission Enhancement in Ce^{3+} /Mn^{2+} Co-Doping Suited Garnet Host $MgY_2Al_4SiO_{12}$ for Tunable Warm White LED. *Opt. Mater.* **2017**, *72*, 257-264.

23. He, X.; Liu, X.; Zhang, Y.; Yu, Y.; Wang, X.; Yu, R., Monitor Local Structure Variation of Ce^{3+} Activator in YAG:Ce Nanophosphor with Calcination Temperature by Nuclear Magnetic Resonance Spectroscopy. *J. Alloy. Compd.* **2017**, *729*, 929-935

24. Gorbenko, V.; Zorenko, T.; Paprocki, K.; Iskaliyeva, A.; Fedorov, A.; Schröppel, F.; Levchuk, I.; Osvet, A.; Batentschuk, M.; Zorenko, Y., Epitaxial Growth of Single Crystalline Film Phosphors Based on the Ce^{3+}-Doped $Ca_2YMgScSi_3O_{12}$ Garnet. *Crystengcomm* **2017**, *19*, 3689-3697

25. Tratsiak, Y.; Bokshits, Y.; Borisevich, A.; Korjik, M.; Vaitkevičius, A.; Tamulaitis, G., $Y_2CaAlGe(AlO_4)_3$:Ce and $Y_2MgAlGe(AlO_4)_3$:Ce Garnet Phosphors for White LEDs. *Opt. Mater.* **2017**, *67*, 108-112.

26. Pan, Y.; Wu, M.; Su, Q., Tailored Photoluminescence of YAG:Ce Phosphor through Various Methods. *J. Phys. Chem. Solids* **2004**, *65*, 845-850.

27. Veith, M.; Mathur, S.; Kareiva, A.; Jilavi, M.; Zimmer, M.; Huch, V., Low Temperature Synthesis of Nanocrystalline $Y_3Al_5O_{12}$ (YAG) and Ce-Doped $Y_3Al_5O_{12}$ Via Different Sol–Gel Methods. *J. Mater. Chem. C* **1999**, *9*, 3069-3079.

28. Zhou, Y.; Lin, J.; Yu, M.; Wang, S.; Zhang, H., Synthesis-Dependent Luminescence Properties of $Y_3Al_5O_{12}$:Re^{3+} (Re=Ce, Sm, Tb) Phosphors. *Mater. Lett.* **2002**, *56*, 628-636.

29. Abd, H. R.; Hassan, Z.; Ahmed, N. M.; Almessiere, M. A.; Omar, A. F.; Alsultany, F. H.; Sabah, F. A.; Osman, U. S., Effect of Annealing Time of YAG:Ce^{3+} Phosphor on White Light Chromaticity Values. *J. Electron. Mater.* **2018**, *47*, 1638-1646.

30. Sang, H. L.; Jung, D. S.; Han, J. M.; Koo, H. Y.; Kang, Y. C., Fine-Sized $Y_3Al_5O_{12}$:Ce Phosphor Powders Prepared by Spray Pyrolysis from the Spray Solution with Barium Fluoride Flux. *J. Alloy. Compd.* **2009**, *477*, 776-779.

31. Hao, D. M.; Lin, H.; Zhou, S. M.; Zhang, S.; Yi, X. Z.; Tang, Y. R., Microstructure Optimization of the Composite Phase Ceramic Phosphor for White LEDs with Excellent Luminous Efficacy. *Opt. Lett.* **2015**, *40*, 5479-5481.

32. Song, Z.; Liu, X.; He, L.; Liu, Q. L., Correlation between the Energy Level Structure of Cerium-Doped Yttrium Aluminum Garnet and Luminescent Behavior at Varying Temperatures. *Mater. Res. Express* **2016**, *3*, 055501.

33. Jia, D.; Wang, Y.; Guo, X.; Li, K.; Zou, Y. K.; Jia, W., Synthesis and Characterization of YAG:Ce^{3+} LED Nanophosphors. *J. Electrochem. Soc.* **2007**, *154*, J1-J4.

34. Katelnikovas, A.; Bareika, T.; Vitta, P.; Jüstel, T.; Winkler, H.; Kareiva, A.; Žukauskas, A.; Tamulaitis, G., $Y_{3-x}Mg_2AlSi_2O_{12}$: Ce Phosphors – Prospective for Warm-White Light Emitting Diodes. *Opt. Mater.* **2010**, *32*, 1261-1265.

35. Odziomek, M.; Chaput, F.; Lerouge, F.; Sitarz, M.; Parola, S., Highly Luminescent Yag:Ce Ultra-Small Nanocrystals, from Stable Dispersions to Thin Films. *J. Mater. Chem. C* **2017**,5 , 12561-12570.

36. Gan, L.; Mao, Z. Y.; Xu, F. F.; Zhu, Y. C.; Liu, X. J., Molten Salt Synthesis of YAG:Ce^{3+} Phosphors from Oxide Raw Materials. *Ceram. Int.* **2014**, *40*, 5067-5071.

37. Chiang, C. C.; Tsai, M. S.; Hsiao, C. S.; Hon, M. H., Synthesis of YAG:Ce Phosphor Via Different Aluminum Sources and Precipitation Processes. *Cheminform* **2006**, *416*, 265-269.

38. Pan, Z.; Xu, Y.; Hu, Q.; Li, W.; Zhou, H.; Zheng, Y., Combination Cation Substitution Tuning of Yellow-Orange Emitting Phosphor $Mg_2Y_2Al_2Si_2O_{12}$:Ce^{3+}. *Rsc Adv.* **2014**, *5*, 9489-9496.

39. Valiev, D.; Han, T.; Vaganov, V.; Stepanov, S., The Effect of Ce^{3+} Concentration and Heat Treatment on the Luminescence Efficiency of Yag Phosphor. *Journal of Physics and Chemistry of Solids* **2018**, *116*, 1-6.

40. Zhang, Y.; Qiao, X.; Wan, J.; Wu, L. A.; Chen, B.; Fan, X., Facile Synthesis of Monodisperse Yag:Ce^{3+} Microspheres with High Quantum Yield Via Epoxide-Driven Sol-Gel Route. *J. Mater. Chem. C, **2017**,5,* 8952-8957.

41. Blasse, G.; Bril, A., A New Phosphor for Flying□Spot Cathode□Ray Tubes for Color Television: Yellow□Emitting $Y_3Al_5O_{12}$–Ce^{3+}. *Appl. Phys. Lett.* **1967**, *11*, 53-55.

42. Saladino, M. L.; Chillura Martino, D.; Floriano, M. A.; Hreniak, D.; Marciniak, L.; Stręk, W.; Caponetti, E., Ce:$Y_3Al_5O_{12}$–Poly(Methyl Methacrylate) Composite for White-Light-Emitting Diodes. *J. Phys. Chem. C* **2014**, *118*, 9107-9113.

43. Wang, Y.; Ding, J.; Wang, Y., $Ca_{2-x}Y_{1+x}Zr_{2-x}Al_{3+x}O_{12}$:$Ce^{3+}$: Solid Solution Design toward the Green Emission Garnet Structure Phosphor for near-Uv Leds and Their Luminescence Properties.

J. Phys. Chem. C **2017**, *121*, 27018-27028.

44. Xia, L.; Ye, X.; Ge, H.; Qiang, Y.; Xiao, Q.; Zhang, Q.; Tong, Z., Erosion Mechanism of YAG:Ce^{3+} Phosphor in Bismuth Borate Glasses. *Ceram. Int.* **2017**, *43*, 17005-17014.

45. Guo, D.; Ma, B.; Zhao, L.; Qiu, J.; Liu, W.; Sang, Y.; Claverie, J.; Liu, H., Bright YAG:Ce Nanorod Phosphors Prepared Via a Partial Wet Chemical Route and Biolabeling Applications. *ACS Appl. Mater. Inter.* **2016**, *8*, 11990-11997.

46. Niu, X.; Xu, J.; Zhang, Y., The Spectroscopic Properties of Dy^{3+} and Eu^{3+} Co-Doped $Y_3Al_5O_{12}$ (YAG) Phosphors for White LED. *Prog. Nat. Sci.* **2015**, *25*, 209-214.

47. Krames, M. R.; Shchekin, O. B.; Mueller-Mach, R.; Mueller, G. O.; Zhou, L.; Harbers, G.; Craford, M. G., Ieee/Osa Status and Future of High Power Light Emitting Diodes for Solid State Lighting. *J. Disp. Technol.* **2007**, *3*, 160-175.

48. Hu, Y.; Zhuang, W.; Ye, H.; Zhang, S.; Fang, Y.; Huang, X., Preparation and Luminescent Properties of $(Ca_{1-x}Sr_x)S:Eu^{2+}$ Red-Emitting Phosphor for White LED. *J. Lumin.* **2005**, *111*, 139-145.

49. Horikawa, T.; Piao, X. Q.; Fujitani, M.; Hanzawa, H.; Machida, K., Preparation of $Sr_2Si_5N_8:Eu^{2+}$ Phosphors Using Various Novel Reducing Agents and Their Luminescent Properties. *IOP Conf. Ser.: Mater. Sci. Eng.* **2009**, *1*, 012024.

TOC:

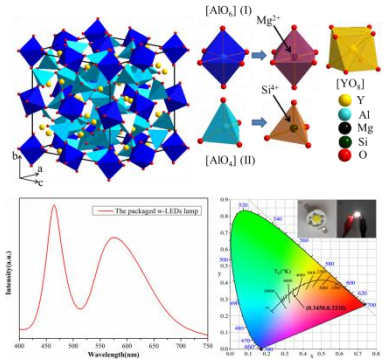
[AlO4] (I)
Mg2+
Si4+
[AlO4] (II)
[YO8]
Y
Al
Mg
Si
O
b
a
c
The packaged w-LEDs lamp
Intensity(a.u.)
Wavelength(nm)
400
450
500
550
600
650
700
750